Optimal Handover Strategies in LEO Satellite Networks

Brendon McBain, *Member, IEEE,* Yi Hong, *Senior Member, IEEE,* and Emanuele Viterbo, *Fellow, IEEE*

Abstract—**Existing theoretical analyses of satellite mega-constellations often rely on restrictive assumptions—such as short serving times—or lack tractability when evaluating realistic handover strategies. Motivated by these limitations, this paper develops a general analytical framework for accurately characterising the ergodic capacity of low Earth orbit (LEO) satellite networks under arbitrary handover strategies. Specifically, we model the transmission link as shadowed-Rician fading and introduce the persistent satellite channel, wherein the channel process is governed by an i.i.d. renewal process under mild assumptions of uncoordinated handover decisions and knowledge of satellite ephemeris and fading parameters. Within this framework, we derive the ergodic capacity (persistent capacity) of the persistent satellite channel using renewal theory and establish its relation to the non-persistent capacity studied in prior work. To address computational challenges, we present closed-form upper and lower bounds on persistent capacity. The optimal handover problem is formulated as a non-linear fractional program, obtaining an explicit decision rule via a variant of Dinkelbach's algorithm. We further demonstrate that a simpler handover strategy maximising serving capacity closely approximates the optimal strategy, providing practical insights for designing high-throughput LEO satellite communication systems.**

I. Introduction

The dynamic architecture of *low-Earth orbit (LEO)* satellite networks presents unique challenges in maintaining continuous and reliable communication, particularly during satellite handovers [1], [2], [3], [4]. The rapid movement of satellites in the mega-constellation necessitates efficient handover strategies that minimise service degradation for communications between LEO satellite networks and ground users. In this context, information-theoretic handover strategies are critical for achieving high-throughput communications in the presence of frequent transitions between serving satellites. This paper provides a comprehensive theoretical analysis of handover strategies that are optimal in the ergodic capacity sense for mega-constellations modelled as semi-stochastic processes.

The communications system model is often based on a time-varying satellite constellation model with satellites serving multiple users within their spotbeams on Earth. This deterministic system model is used in simulation-based analyses for an accurate description of the performance of a particular system. However, it poses some tractability issues when it comes to theoretical analysis, especially for ultra-dense LEO

mega-constellations that nowadays typically have hundreds or even thousands of satellites [5]. Taking advantage of the large number of satellites in an ultra-dense mega-constellation, stochastic system models have been developed in recent years to model satellite mega-constellations using point processes [6], [7]. While stochastic models are limited in their ability to accurately capture time-dependent orbit trajectories over short time scales, they offer tractable system models that are amenable to theoretical analyses which describe the system performance with more generality. The loss in accuracy of stochastic models can be reduced using our semi-stochastic model [8], which recovers the time-dependent behaviour of the orbit trajectories while retaining tractability. The essence of our approach is to consider the orbital trajectories of only the satellites visible at the handover decision time, improving tractability while maintaining high accuracy. A key open question concerns the choice of modelling framework—deterministic, stochastic, or semi-stochastic—depending on the purpose of the analysis, such as performance characterisation or communication strategy design (e.g., handover optimisation). In many cases, incorporating the system's time-dependent behaviour is essential; otherwise, the resulting analysis would be inherently limited.

A critical aspect of satellite mega-constellation networks is the *handover strategy* that determines which satellite from the mega-constellation will serve the ground user and for how long. For ultra-dense mega-constellations, there are typically tens of visible satellites that are candidates for serving the user. Exploiting this satellite diversity, the system has the unique ability to choose the user-satellite channel through the handover decision. In addition, the next handover decision is made according to the handover trigger, which is an event that triggers a handover decision on the candidate satellites at the current moment. Therefore, the handover strategy, which specifies the handover decision rule and the handover trigger, is critical to the system performance.

For example, the handover decision rule may be to choose the satellite with the minimum distance (maximum elevation angle) since it minimises path loss and propagation delay, and the handover trigger may be the event that the serving satellite is no longer visible (below the minimum elevation angle) since the lack of a line-of-sight significantly degrades the channel. In [9], Voicu et al. conducted an empirical analysis of this strategy in terms of capacity, propagation delay, and Doppler shift. Motivated by this example, handover strategies are typically designed to follow Papapetrou's criteria [10]:

1) *Maximum serving time*: Choose the satellite with the longest serving time to avoid frequent satellite handover;

2) *Minimum distance*: Choose the nearest satellite, as it provides the lowest path-loss and propagation delay;
3) *Maximum number of free channels*: Choose the satellite with the largest number of free channels to balance the network load.

In our earlier example, the decision rule was based on Criterion 2 and the trigger was based on Criterion 1. However, choosing the nearest satellite as in Criterion 2 does not always yield the most reliable user-satellite channel in the presence of shadowing. In addition, since this criterion is only in action at the handover time, it does not capture the time-dependent evolution of the user-satellite channel up until the handover trigger; if the serving times are long enough to allow for large variations in reliability, such a handover decision rule is unlikely to be optimal in aggregation. Observe that since Criterion 3 necessarily involves a multi-user scenario with limited resources, handover strategies that include this criterion often lose tractability due to dependencies between users [11]. While this does not directly affect system performance, it does limit the ability to evaluate and optimise handover strategies.

In [12], Okati and Riihonen formally introduced the notion of an optimal handover strategy as the strategy that maximises the received SNR, indirectly maximising ergodic capacity. In [13], Guo et al. introduced analogous handover strategies for multi-tier mega-constellations. This addressed the limitations regarding Criterion 2 and Criterion 3 of Papapetrou's criteria; the limitation regarding Criterion 1 was not addressed, which is an inherent limitation to using purely stochastic models that do not include time. Moreover, a special case of the proposed analytical framework will show that stochastic models are only applicable to scenarios with short serving times. In particular, the existing frameworks based on stochastic models will be generalised to a semi-stochastic model to enable the study of arbitrary (long) serving times using our so-called *persistent (satellite) capacity* [8]. In this setting, the optimal handover decision rule that maximises persistent capacity requires satellite orbit prediction in order to compute the serving capacity of candidate satellites, as in [14], [15].

A. Contributions

Motivated by the lack of generality in previous theoretical analyses and the lack of tractability in empirical analyses, we provide a theoretical framework for accurately analysing the ergodic capacity of satellite mega-constellation networks with general handover strategies. Within this framework, we are able to derive the optimal handover strategy. The main contributions of this paper are summarised as follows:

- We develop an analytical framework based on semi-stochastic modelling [8] (extending the analytical framework based on stochastic modelling [7], [16]) for analysing generalised handover strategies employed by a ground user for communications with a LEO satellite network. The transmission link is modelled as shadowed-Rician fading, and the satellite mega-constellation is modelled as a *non-homogeneous binomial point process (NBPP)* that initialises a deterministic circular orbit

trajectory. Under the assumption that consecutive handover decisions are made independently and the handover strategy has knowledge of the satellite ephemeris data and the shadowed-Rician fading parameters, the channel process is governed by an i.i.d. renewal process. Since this channel model captures the time-varying behaviour of the link while a satellite persistently serves the ground user, we refer to it as the *persistent satellite channel*.

- The ergodic capacity of the persistent satellite channel (the persistent capacity) is derived from the renewal theorem. The persistent capacity—which depends on the handover strategy—is related to the *non-persistent capacity* from the literature [17] by enforcing a maximum serving time that approaches zero. Since the persistent capacity is challenging to compute for arbitrary handover strategies, we derive closed-form upper and lower bounds. The upper bound corresponds to the maximum serving capacity that is possible, and the lower bound is the persistent capacity with the random handover strategy, which can be computed numerically [8]. In addition, we show that the non-persistent capacity is an approximate upper bound on the persistent capacity, suggesting that we should choose short serving times if the system constraints allow it.

- We formally define the optimal handover strategy as the strategy that maximises the persistent capacity. Since the persistent capacity is essentially the ratio of the sum of serving capacities and the sum of serving times, the maximum persistent capacity and its corresponding optimal handover strategy can be found using a variation of Dinkelbach's algorithm for non-linear fractional programs. This results in a remarkably simple handover decision rule that depends on a satellite's serving capacity and serving time, and the persistent capacity achieved by employing this strategy. In addition, we tightly approximate the optimal handover strategy with a handover strategy that maximises serving capacity, which does not require knowledge of the maximal persistent capacity.

B. Notation

A random variable is denoted by a capital letter such as X. The probability density of X is denoted by $f_X(x)$ for $x \in \mathbb{R}$. The expectation of $g(X)$, for some function g, is $\mathbb{E}[g(X)] = \int_{\mathbb{R}} g(x)f_X(x)dx$. For functions of multivariate random variables, e.g., X and Y, we denote the expectation with respect to X as $\mathbb{E}_X[g(X,Y)]$ where Y is being conditioned on. The i.i.d. continuous uniform random variable is denoted by $\mathcal{U}(\mathcal{A})$ with compact support $\mathcal{A} \subset \mathbb{R}$. The base-2 logarithm is denoted by $\log$.

II. MODELLING SATELLITE MEGA-CONSTELLATIONS

A. Visibility Cap of Ground User

The visible region of satellites above a user may be obstructed by obstacles, or it may be limited for interference mitigation. Hence, it is common to specify a minimum elevation angle $\psi_{\min}$ relative to the horizon of the user, above which a satellite is assumed to be visible and able to serve
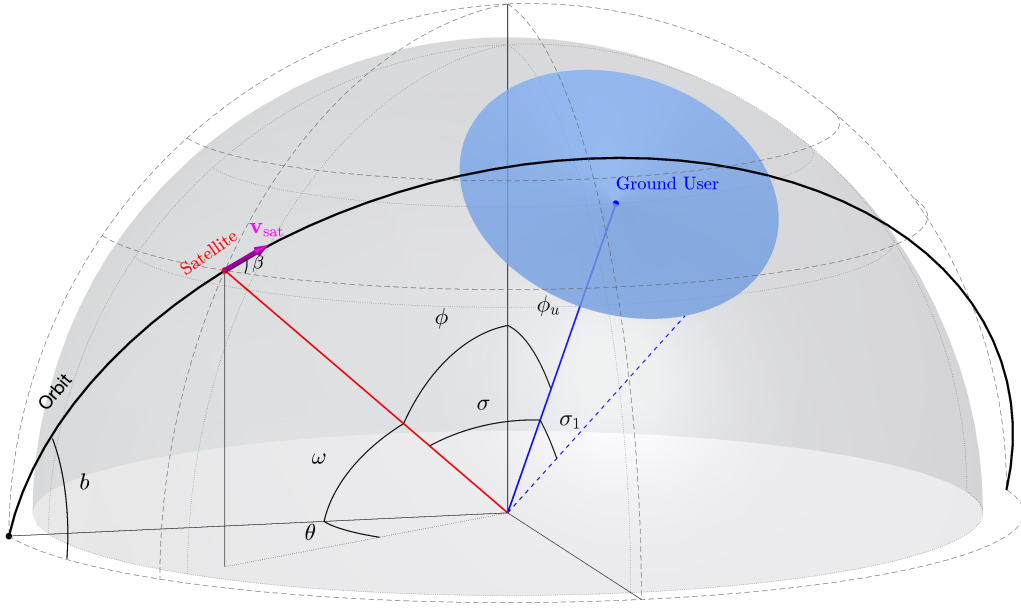
Figure 1: A satellite on an orbit towards the visibility cap of a ground user.

the user. This minimum elevation angle also corresponds to a cone with maximum central angle σ_1. Consider a user at (r, θ_u, ϕ_u) and a satellite at (R, θ, ϕ), and let the central angle between them be $\sigma = \sigma(\theta, \phi)$ given by

$$\sigma = \cos^{-1}\big(\cos\phi_u \cos\phi + \sin\phi_u \sin\phi \cos(\theta_u - \theta)\big). \quad (1)$$

Then, the region of visible satellites forms a cap on the satellite sphere given by the region

$$\mathsf{Cap} = \{(\theta, \phi) : 0 \leq \theta \leq 2\pi, \sigma(\theta, \phi) \leq \sigma_1\}. \quad (2)$$

In addition, we can re-parameterise the cap by solving $\sigma(\theta, \phi) = \sigma_1$ for θ in terms of ϕ, which has the two solutions $\theta_L(\phi) = \theta_u - L(\phi)/2$ and $\theta_U(\phi) = \theta_u + L(\phi)/2$, where $L(\phi)$ is the arc length of the latitude line on the cap with polar angle ϕ and is given as

$$L(\phi) = \pi + 2\sin^{-1}\big(\csc\phi\big(\cot\phi_u \cos\phi \\ - \cos\sigma_1 \csc\phi_u\big)\big). \quad (3)$$

Hence, now we have

$$\mathsf{Cap} = \big\{(\theta, \phi) : \theta_L(\phi) \leq \theta \leq \theta_U(\phi), 0 \leq \phi \leq \pi\big\}, \quad (4)$$

which is a useful parameterisation since it is written directly in terms of θ and ϕ rather than in terms of the central angle $\sigma(\theta, \phi)$.

B. Deterministic Model

1) Circular Orbits: Consider a LEO orbit at altitude h around a static and spherical Earth of radius r. A satellite is moving along this orbit on a satellite sphere of radius $R = r + h$ as illustrated in Fig. 1. The *argument of latitude* ω is the angle of the satellite on the orbital plane, relative to the *ascending node* that intersects the equatorial plane of Earth and corresponds to $\omega = 0$. At the ascending node, the orbital plane is tilted away from the equatorial plane

by orbital inclination angle b. When $\omega < \pi$ the satellite is ascending, and when $\omega > \pi$ the satellite is descending. The satellite is moving at a constant speed v_{sat}, resulting in angular velocity $\omega_{\text{sat}} = v_{\text{sat}}/R$ and orbital period $T_{\text{sat}} = 2\pi/\omega_{\text{sat}}$. The direction of the velocity vector of the satellite and the latitude line at ϕ is $\beta_a(\phi) = a\cos^{-1}(\cos(b)/\sin(\phi))$ where $a = +1$ if ascending or $a = -1$ if descending. Satellite mega-constellations are composed of multiple orbital planes with ascending nodes spaced by angle s_{orb}, and each orbital plane contains N_{orb} uniformly distributed satellites. The total number of satellites is $N_{\text{sat}} = 2\pi N_{\text{orb}}/s_{\text{orb}}$.

The position of a satellite on a circular orbit as described can be computed using a sequence of rotations around the x-axis, y-axis, and z-axis in a cartesian coordinate system using rotation matrices $R_x(\cdot)$, $R_y(\cdot)$, and $R_z(\cdot)$, respectively. Starting at initial position $(R, \theta(0), \phi(0))$, the satellite follows a deterministic orbit trajectory with time-dependent positions $(R, \theta(t), \phi(t))$ and is ascending/descending according to a. Hence, the angle between the direction vector of the satellite and the latitude line at $\frac{\pi}{2} - \phi(0)$ is $\beta_a(\phi(0)) = a\cos^{-1}(\cos(b)/\sin(\phi(0)))$. These positions can be computed in cartesian coordinates as follows:

1) Initialise the satellite on a flat orbital plane at spherical coordinates $(R, \omega_{\text{sat}}t, 0)$;
2) Rotate counter-clockwise around the x-axis by satellite direction $\beta_a(\phi(0))$ radians;
3) Rotate clockwise around the y-axis by latitude $\frac{\pi}{2} - \phi(0)$ radians;
4) Rotate counter-clockwise around the z-axis by longitude $\theta(0)$ radians;

and then convert from cartesian coordinates to the spherical coordinates $(R, \theta(t), \phi(t))$. Hence, the time-dependent distance between a user and the satellite is $d(t) = d(\theta(t), \phi(t))$ and their time-dependent central angle is $\sigma(t) = \sigma(\theta(t), \phi(t))$. In addition, the satellite only has a line-of-sight with the user

for a visibility time $T(\theta(0), \phi(0), a)$, in seconds, and is the time it takes for the elevation angle of the satellite to equal the minimum elevation angle $\psi_{\min}$ (or maximum central angle σ_1). Formally, this can be found by finding the root of $\sigma(t) - \sigma_1$ over domain $t \in [0, T_{\text{sat}}/2]$, noting that this domain excludes the root on the other side of the visibility cap of satellites.

2) SGP4 Orbits: Realistic simulations can be performed using the *Simplified General Perturbations 4 (SGP4)* orbit model that considers perturbations (e.g., due to Earth's shape, drag, radiation, and gravitation effects from the sun and the moon) that cause the satellites to deviate from their average circular orbits. With this model, realistic orbits can be simulated using a *two-line element (TLE)* file of the constellation.

C. Stochastic Model

We now leverage the fact that there are a large number of satellites in a LEO mega-constellation, so that we can stochastically model the satellite positions using a point process. The uniformly spaced ascending nodes are stochastically modelled as a continuous uniform variable, such that the rotational angle (longitude) of a satellite is a random variable

$$\Theta \sim \mathcal{U}([0, 2\pi]). \tag{5}$$

The uniformly spaced satellites on an orbital plane are stochastically modelled as a continuous uniform random variable for the argument of latitude, resulting in a polar angle Φ with PDF (as derived in [17, Lemma 2] for latitude $\pi/2 - \phi$)

$$f_\Phi(\phi) = \frac{\sin(\phi)}{\pi\sqrt{\sin^2(\phi) - \cos^2(b)}} \tag{6}$$

for $\phi \in [\bar{b}, \pi - \bar{b}]$ and zero otherwise. Thus, the positions of the N_{sat} satellites in the mega-constellation are i.i.d. stochastically modelled as the spherical coordinates (R, Θ, Φ), forming an NBPP on a sphere. The NBPP is an accurate model for the first-order statistics of the positions of satellites in a mega-constellation, assuming the orbital spacing s is small and the satellites spend equal durations at all longitudes and all arguments of latitude. In addition, we mark the satellite positions in the NBPP with a uniform binary variable A that specifies whether the satellite is ascending $(+1)$ or descending (-1) on its orbit, which is the sign of direction angle $\beta_A(\Phi)$.

Since we are often interested in the influence of the mega-constellation on a ground user, we can form a user-centric stochastic model by defining the random set of N_{vis} visible satellites as $\mathcal{V} = \{(\Theta_1, \Phi_1), (\Theta_2, \Phi_2), \cdots\}$ with respect to a user at $(r, \theta_{\text{u}}, \phi_{\text{u}})$. Observe that in the stochastic model there is a non-zero probability that we have the event $N_{\text{vis}} = 0$, which would not actually be possible in a real mega-constellation designed for full ground coverage; hence, we include the condition $N_{\text{vis}} \geq 1$ in the model.

III. PERSISTENT SATELLITE CHANNEL

The information-bearing signal $x(t)$ is transmitted by a serving satellite $(\Theta_0, \Phi_0, A_0) \in \mathcal{V}$ with orbit trajectory $(R, \Theta_0(t), \Phi_0(t))$ and is received as $y(t)$ by a fixed ground user at $(r, \theta_{\text{u}}, \phi_{\text{u}})$[1]. Co-channel interference from terrestrial or

[1]Without loss of generality, the transmission link can be considered as either the uplink or the downlink.

non-terrestrial networks is assumed mitigated to an acceptable noise level N_0. The line-of-sight (LOS) signal propagates over a free-space distance $d(\Theta_0(t), \Phi_0(t))$, with path loss proportional to d^{-2}, assumed known via ephemeris data.

Shadowing effects arise from atmospheric phenomena (e.g., rain, clouds, ionospheric scintillation) and local obstructions, while scattering induces non-line-of-sight multipaths. Assuming coherent detection, the resulting fading follows a shadowed-Rician model [18], characterised by the scattering power $2b_0$, Nakagami parameter m, and LOS power Ω, forming time- and space-varying fading parameters $S(\theta, \phi, t) = (b_0, m, \Omega)$. These parameters are assumed to be known at the receiver over the serving time, e.g., via weather data or channel estimation under static or slow-moving conditions.

The satellite mega-constellation channel includes two processes:

1) *Handover process*: Selects a satellite from $\mathcal{V}$ based on position, direction, and predicted fading parameters S, and is modelled as a stochastic point process.
2) *Propagation process*: Models signal propagation between the user and serving satellite as an AWGN channel with time- and space-varying coefficients for path loss and shadowed-Rician fading.

Since these two processes are repeated consecutively, they form a *semi-stochastic continuous-time renewal process*. After discretisation, we have a *discrete-time renewal process* that is used to form a channel model for practical satellite communication systems.

A. Handover Process

The handover process in satellite mega-constellation networks involves selecting the best available channel from the visible satellites for a specific *serving period*, with decisions made by the *central control unit (CCU)*. The CCU uses known satellite position trajectories and fading parameters, denoted by $\{(\Theta_k(t), \Phi_k(t))\}$ and S, respectively. However, it cannot predict small-scale multipath fading or the realisations of large-scale shadowing, only their statistical parameters.

To reduce complexity and memory requirements at the receiver, handover decisions are made independently at each handover event. The receiver must also have access to the same channel state information as the CCU to realise the intended performance gains.

The handover trigger is determined by the *serving time*, which is constrained by:

- A minimum serving time $T_{\min}$, imposed by practical considerations such as latency spikes and network congestion. If a satellite's visible time is less than $T_{\min}$, it is considered to go dark once it is no longer visible (though constellations may be designed to avoid this scenario).
- A maximum serving time $T_{\max}$, which allows more frequent handovers and better satellite selection, improving quality of service.

This is equivalent to computing the serving time by applying a clamping function to the satellite's visible orbit time. Given all of the above, we can formalise the definition of a handover strategy as follows.

Definition 1 (Handover strategy). *A handover strategy* H *is a function that maps a set of visible satellites* $V = \{(\theta_1, \phi_1, a_1), (\theta_2, \phi_2, a_2), \ldots, (\theta_N, \phi_N, a_N)\}$ *and shadowing parameters* S *to a serving satellite as* $\mathsf{H}(V, S) = (\theta_k, \phi_k, a_k) \in V$ *with serving time* $\mathsf{T}(\theta_k, \phi_k, a_k) = \min\{\max\{\mathsf{T}_{\mathrm{vis}}(\theta_k, \phi_k, a_k), T_{\min}\}, T_{\max}\}$.

B. Propagation Process

The propagation process is initialised with a handover strategy H applied to the visible satellites $\mathcal{V}$ to get the orbit intialisation $(\Theta_0, \Phi_0, A_0) = \mathsf{H}(\mathcal{V}, S)$, which is then used to determine the time-varying channel conditions along the orbit trajectory, while data is transmitted during the serving time.

The communication link between the user and satellite is modelled as a discrete-time fading AWGN channel with large-scale path-loss and small-scale shadowed-Rician fading. The satellite positions are assumed to be constant within a coherence time Δt seconds of the path-loss, and the shadowed-Rician coefficients are assumed to be constant within a coherence time of T_s seconds. In practice, we have that $T_s \ll \Delta t$ since the satellite movement is relatively slow compared to the fast-fading. During the serving time $T_{\mathrm{serv}} = \mathsf{T}(\mathcal{V}, S)$, we transmit frames of duration Δt seconds equal to the coherence time of the path loss. The resulting number of frames is $N_{\mathrm{serv}} = \mathsf{N}(\mathcal{V}, S) = \lfloor \mathsf{T}(\mathcal{V}, S)/\Delta t \rfloor$. The maximum number of frames is $N_{\max} = \lfloor T_{\max}/\Delta t \rfloor$ and the minimum number of frames is $N_{\min} = \lfloor T_{\min}/\Delta t \rfloor$. The discretised channel output for the j-th symbol in the i-th frame is

$$y_{i,j} = \frac{h_{0,i,j}}{\sqrt{\ell_{0,i}}} x_{i,j} + n_{0,i,j} \tag{7}$$

for all $j = 0, 1, \ldots, \lfloor \Delta t/T_s \rfloor - 1$ and $i = 0, 1, \ldots, N_{\mathrm{serv}} - 1$, where:

- $x_{i,j}$ is the complex-valued channel input at time $t = i\Delta t$ with average power equal to the transmit SNR[2] γ;
- $\ell_{0,i,j} = d^2(\Theta_0(i\Delta t + jT_s), \Phi_0(i\Delta t + jT_s))$ is the free-space LOS path loss;
- $h_{0,i,j}$ is an i.i.d. complex-valued shadowed-Rician process with ergodic fading parameters $S(\Theta_0, \Phi_0, i\Delta t + jT_s)$;
- $n_{0,i,j}$ is an i.i.d. complex-valued AWGN noise process with unit power.

Note: For notational convenience, the fading coefficients $h_{0,i,j}$ are i.i.d. $h_{0,i,1} = h_{0,i}$, which depends on the serving satellite, and the noise realisations $n_{0,i,j}$ are i.i.d. $n_{0,i,1} = n_i$, which do not depend on the serving satellite. Without loss of generality, this notation will be used in the next section.

After the serving time has ended, the handover process specifies a new serving satellite and the above process repeats as in an i.i.d. renewal process.

We note that the model could be extended in several ways—for instance, by incorporating memory across frames when shadowing correlation persists over several seconds, or by accounting for user-satellite interference. However, since the

subsequent handover strategy analysis depends primarily on the renewal property of the channel, such extensions are omitted for simplicity. In essence, we focus on the model assumptions that directly affect the handover strategy.

C. Non-Persistent Satellite Channel

An interesting special case of the previously defined satellite channel, which models persistent communications, is when the maximum serving time $T_{\max}$ is reduced. As $T_{\max} \to \Delta t$, resulting in $T_{\mathrm{serv}} \to \Delta t$, transmission only occurs over the initial frame at $i = 0$, since $N_{\mathrm{serv}} = 1$. The channel output is therefore

$$y_{0,0} = \frac{h_{0,0}}{\sqrt{\ell_{0,0}}} x_{0,0} + n_0. \tag{8}$$

Notice that this case completely ignores the part of the propagation process that predicts the orbit trajectory and thus it corresponds to non-persistent communications. Moreover, the semi-stochastic model becomes a purely stochastic model with instantaneous handovers, demonstrating that the persistent channel is a generalisation of the non-persistent channel.

IV. PERSISTENT SATELLITE CHANNEL CAPACITY

A. Ergodic Capacity: The SatCom Interpretation

Since the ergodic capacity of a persistent satellite channel cannot be evaluated using the typically used formula for ergodic capacity, this section is dedicated to setting up the definition and intuition behind the ergodic capacity for satellite mega-constellations with persistence.

Consider a serving period consisting of N_{serv} frames. Within each frame i, the path loss $\ell_{0,i}$ is constant, while the fading coefficient $h_{0,i}$ and noise realisation n_i vary independently across frames. The achievable rate per frame is

$$W_i = \mathbb{E}_{|h_{0,i}|^2}\left[\log\left(1 + \frac{\gamma|h_{0,i}|^2}{\ell_{0,i}}\right)\right]\Delta t. \tag{9}$$

Let $W(t)$ denote the total transmitted data in a session of duration t seconds. As the system undergoes successive handovers, each serving period can be viewed as one renewal, with the total transmitted data per period,

$$W_{\mathrm{serv}} = \sum_{i=0}^{N_{\mathrm{serv}}-1} W_i,$$

representing the reward.

By the renewal reward theorem, the long-term average (ergodic) capacity is

$$C_{\mathrm{ergodic}} = \lim_{t\to\infty} \frac{W(t)}{t} = \frac{\mathbb{E}[W_{\mathrm{serv}}]}{\mathbb{E}[N_{\mathrm{serv}}\Delta t]}, \tag{10}$$

in bits per second.

Thus, the ergodic capacity equals the ratio of the average transmitted data per serving period (bits per serve) to the average duration per serving period (seconds per serve). Since Δt cancels out, an equivalent discrete-time formulation can be used without loss of generality.

---

[2]This parameter is independent of any specific system parameters contributing to the path loss (bandwidth, wavelength, antenna gains, distance), which we can ignore in our theoretical analysis.

Finally, let us highlight the assumptions behind the ergodic capacity C_{ergodic} in the scenario of satellite mega-constellation communications:

1) No power allocation is performed at the transmitter, resulting in a fixed transmit SNR γ;
2) The transmitter and receiver know the path loss $\ell_{0,i}$ using ephemeris data;
3) The receiver knows the fading coefficient $h_{0,i}$ through channel estimation;
4) Optimal rate adaptation (ORA) is employed to adjust the coding rate to each instantaneous capacity W_i;
5) Δt is a sufficiently long delay[3] to reliably transmit data at rates close to each instantaneous capacity W_i.

Next, we will apply this capacity to the persistent satellite channel model from the previous section, where the rewards are determined by the shadowed-Rician fading parameters and the average of their sum is determined by the NBPP.

B. Persistent Capacity

The capacity of the persistent satellite channel, conditioned on any satellite $(\Theta_k, \Phi_k, A_k) \in \mathcal{V}$ to serve the user for N_{serv} frames, is a sum-rate of independent AWGN fading channels with path losses $\{\ell_{k,i}\}$ (which depends on the orbit trajectory $\{\Theta_{k,i}, \Phi_{k,i}\}$) and shadowed-Rician coefficients $\{h_{k,i}\}$. Therefore, the total capacity over the serving time is

$$\mathsf{C}(\Theta_k, \Phi_k, A_k) = \sum_{i=0}^{\min\{N_{\max}, N_{\text{vis}}\}-1} C_{k,i}, \qquad (11)$$

where, with shadowed-Rician fading, the instantaneous capacities can be efficiently evaluated as [19]

$$C_{k,i} = \mathbb{E}_{|h_{k,i}|^2}\left[\log\left(1 + \frac{\gamma|h_{k,i}|^2}{\ell_{k,i}}\right)\right]$$
$$= \frac{1}{\ln 2}\int_0^\infty E_i\left(-\frac{s\ell_{k,i}}{\gamma}\right) M^{(1)}(s)ds, \qquad (12)$$

where E_i is the exponential integral function and $M^{(1)}(s)$ is the first derivative of the shadowed-Rician MGF given by

$$M^{(1)}(s) = b_0(b_0 m)^m (1 + 2b_0 s)^{m-2} \cdot$$
$$\frac{4b_0^2 ms + m\Omega + 2b_0(m + s\Omega)}{[b_0(m + 2b_0 ms + s\Omega)]^{m+1}}. \qquad (13)$$

Note that this capacity is independent of the handover strategy since we conditioned on an arbitrary serving satellite.

Let us now average the total capacity with respect to the distribution of the serving satellite, which does depend on the handover strategy, and divide by the average serving time to get the capacity of the persistent satellite channel.

Theorem 1 (Persistent capacity). *The ergodic capacity of the persistent satellite mega-constellation channel with handover strategy* H *is*

$$C_{\text{pers}}[\mathsf{H}] = \frac{\mathbb{E}_{\mathcal{V},S}[\mathsf{C}(\mathsf{H}(\mathcal{V}, S))]}{\mathbb{E}_{\mathcal{V},S}[\mathsf{N}(\mathsf{H}(\mathcal{V}, S))]} \qquad (14)$$

---

where $\mathcal{V}$ *is the set of visible satellites from the mega-constellation NBPP with* $|\mathcal{V}| \geq 1$.

Proof. This is a consequence of the renewal reward theorem for renewal reward processes as demonstrated in Section IV-A. $\qquad \square$

Remark 1. *The proof of Theorem 1 is simple to show for the special case where we let the session time* t *coincide with the duration of exactly* N *handovers. If we let* $\{\mathcal{V}^{(n)}\}$ *be the random sets of visible satellites at the handovers* $n = 1, 2, \ldots, N$, *which are i.i.d. realisations of the mega-constellation NBPP, then the achievable data rate is*

$$\frac{\sum_{n=1}^N \mathsf{C}(\mathsf{H}(\mathcal{V}^{(n)}, S))}{\sum_{n=1}^N \mathsf{N}(\mathsf{H}(\mathcal{V}^{(n)}, S))} \to C_{\text{pers}}[\mathsf{H}] \qquad (15)$$

as $N \to \infty$ *due to the strong law of large numbers. When* t *is arbitrary, we must additionally account for the capacity of the possibly incomplete final serving period. However, since this capacity is bounded, it does not change the limit and the result above remains.*

We remark that while persistent capacity obeys the general form of ergodic capacity [20], which allows for time-dependence so long as the channel state process is ergodic, it is different to the standard ergodic capacity formula used in the wireless communications literature that averages $\log(1 + \mathsf{SNR})$ with respect to a random variable SNR. In the following section, we consider a special case of the persistent capacity which coincides with the typical ergodic capacity from the literature.

C. Non-Persistent Capacity

The capacity of the persistent satellite channel (persistent capacity) as $T_{\max} \to 0$ yields the capacity of the non-persistent satellite channel (non-persistent capacity). Hence, we have the following corollary of Theorem 1, which is the capacity used in the stochastic analysis of handover strategies in [12] with the condition $|\mathcal{V}| \geq 1$.

Corollary 1 (Non-persistent capacity). *The non-persistent capacity of a satellite mega-constellation with handover strategy* H *is*

$$C_{\text{non-pers}}[\mathsf{H}] = \mathbb{E}\left[\log\left(1 + \frac{\gamma|h_{0,0}|^2}{d^2(\Theta_0, \Phi_0)}\right)\right] \qquad (16)$$

where $(\Theta_0, \Phi_0, \cdot) = \mathsf{H}(\mathcal{V}, S)$.

The non-persistent capacity is an interesting special case of the persistent capacity since it is an approximate upper bound. This can explained using a property of mutual information $I(\mathbf{x}; \mathbf{y})$ between the channel inputs $\mathbf{x} = [x_{0,1}, x_{0,2}, \ldots, x_{0,N_{\text{serv}}-1}]^\top$ and outputs $\mathbf{y} = [y_{0,1}, y_{0,2}, \ldots, y_{0,N_{\text{serv}}-1}]^\top$, ignoring CSI for simplicity, for channels with stationary state processes that satisfy $I(x_{0,0}; y_{0,0}) = I(x_{0,i}; y_{0,i})$ for all i. For such channels, we have the inequality [21]

$$I(\mathbf{x}; \mathbf{y}) \leq N_{\text{serv}} I(x_{0,0}; y_{0,0}) \qquad (17)$$

where maximising both sides with respect to the channel inputs gives their respective capacities. In the case of the persistent satellite channel, we have the approximation $I(x_{0,0}; y_{0,0}) \approx I(x_{0,i}; y_{0,i})$ whose accuracy depends on how accurately the NBPP models the satellite positions in the deterministic mega-constellation orbits at handover events. As it turns out, it is a very good approximation and serves as an accurate upper bound on the persistent capacity for a given handover strategy.

D. Upper Bound on Persistent Capacity

The persistent capacity $C_{\text{pers}}[\mathsf{H}]$ depends on the handover strategy H that is chosen. In the next section, we will derive the handover strategy that maximises this capacity. However, since numerically computing $C_{\text{pers}}[\mathsf{H}]$ is difficult in general, due to the order statistics often required to describe a handover strategy, it is useful to at least have capacity bounds that can be numerically computed. The following proposition provides a closed-form upper bound that is independent of the handover strategy. We note that this upper bound cannot be achieved by any realisable handover strategy. In the next section, we will pair this upper bound with a lower bound based on the worst-case handover strategy.

Proposition 1. *For an arbitrary handover strategy* H*, which need not obey Definition 1, we have the upper bound*

$$\overline{C}_{\text{pers}} = \max_{a \in \{-1,+1\}} \sup_{(\theta,\phi) \in \mathsf{Cap}} \left\{ \frac{\mathsf{C}(\theta, \phi, a)}{\mathsf{N}(\theta, \phi, a)} \right\} \quad (18)$$

that satisfies $C_{\text{pers}}[\mathsf{H}] \leq \overline{C}_{\text{pers}}$.

Proof. Observe that the function $f(x,y) = x/y$ is convex in x, y if $x \geq 0$ and $y > 0$. In addition, observe that $\mathsf{C}(\theta, \phi, a) \geq 0$ since information rates must be positive, and $\mathsf{N}(\theta, \phi, a) > 0$ since there must be at least 1 frame per serve. Then, we employ the two-variable version of Jensen's inequality that says

$$f(\mathbb{E}[(\mathsf{C}(\Theta_0, \Phi_0, A_0), \mathsf{N}(\Theta_0, \Phi_0, A_0))])$$
$$\leq \mathbb{E}[f(\mathsf{C}(\Theta_0, \Phi_0, A_0), \mathsf{N}(\Theta_0, \Phi_0, A_0))] \quad (19)$$

where, by monotonicity of expectation, the right-hand side is further upper bounded by the maximum over the support of the function. $\quad\square$

V. Optimal Handover Strategy

For a fixed handover strategy H, the persistent capacity was derived in Theorem 1 as the maximum achievable rate. We now consider the maximisation of persistent capacity with respect to the handover strategy to find the optimal handover strategy.

Definition 2 (Optimal handover strategy). *The handover strategy* H^* *is optimal if*

$$C_{\text{pers}}[\mathsf{H}^*] = \sup_{\mathsf{H} \in \mathcal{H}} C_{\text{pers}}[\mathsf{H}] \quad (20)$$

where $\mathcal{H}$ *is the set of all handover strategies that satisfy Definition 1.*

A. Dinkelbach's Algorithm

For convenience, denote $C_{k,n}$ as the total capacity, $N_{k,n}$ as the number of frames in the serving period, and $p_{k,n}$ as a binary variable indicating the handover decision, at the n-th handover event of the k-th visible satellite in $\mathcal{V}^{(n)}$. Define the vectors $\mathbf{C}_n = [C_{1,n}, \ldots, C_{|\mathcal{V}^{(n)}|,n}]^\top$, $\mathbf{N}_n = [N_{1,n}, \ldots, N_{|\mathcal{V}^{(n)}|,n}]^\top$, and $\mathbf{p}_n = [p_{1,n}, \ldots, p_{|\mathcal{V}^{(n)}|,n}]^\top$. Then, the normalised capacity can be expressed compactly as

$$C_N(\mathbf{p}) = \frac{\sum_{n=1}^N \mathbf{p}_n^\top \mathbf{C}_n}{\sum_{n=1}^N \mathbf{p}_n^\top \mathbf{N}_n} = \frac{U_N(\mathbf{p})}{V_N(\mathbf{p})}, \quad (21)$$

and then solving for the optimal handover decisions $\mathbf{p}$ is the 0-1 fractional program [22]

$$C^* = \max_{\mathbf{p} \in \mathcal{P}} C_N(\mathbf{p}), \quad (22)$$

where $\mathcal{P} = \{\mathbf{p} = (\mathbf{p}_1, \ldots, \mathbf{p}_N) : \mathbf{p}_n \in \{0,1\}^{|\mathcal{V}^{(n)}|}, \mathbf{1}^\top \mathbf{p}_n = 1 \text{ for all } n\}$. While this is a non-convex program in general, Dinkelbach's algorithm ([23], Algorithm 1) transforms it into a sequence of convex programs whose solutions converge to the global optimum. In particular, the Dinkelbach transform replaces the maximisation of the non-convex objective $C_N(\mathbf{p})$ with the maximisation

$$F_N(C) = \frac{1}{N} \max_{\mathbf{p} \in \mathcal{P}} \{U_N(\mathbf{p}) - C V_N(\mathbf{p})\}, \quad (23)$$

where C is an initial guess of the maximum capacity C^* at the global optimum $\mathbf{p}^*$. After solving $F_N(C)$ with some guess C to get a solution $\mathbf{p}$, the guess is updated as $C_N(\mathbf{p})$. Dinkelbach showed that $F_N(C)$ monotonically decreases until $U_N(\mathbf{p}) - C V_N(\mathbf{p}) = 0$ is satisfied, then $C = C^*$ and $\mathbf{p} = \mathbf{p}^*$.

Observe that the handover decisions $\mathbf{p}$ are general in that they do not necessarily correspond to a valid handover strategy as in Definition 1, which only allows memoryless handover decisions. This could result in an undefined capacity since the processes $\{U_N(\mathbf{p}^*)\}$ and $\{V_N(\mathbf{p}^*)\}$ need not be ergodic and consequently $C_N(\mathbf{p}^*)$ may not converge to the persistent capacity in Theorem 1 as $N \to \infty$. This issue will be addressed by modifying Dinkelbach's transform.

The time-complexity of the standard Dinkelbach algorithm, shown in Algorithm 1, has been extensively analysed. In [22], the number of iterations required for 0–1 fractional programs is $O(\log N)$ iterations, corresponding to *superlinear* convergence. Consequently, the dominant computational cost arises from the integer linear-program solver executed at each iteration, scaled by the number of iterations to give the overall time-complexity.

Algorithm 1 Dinkelbach's algorithm

1: Set $C = C_0$ as an initial guess C_0.
2: Solve the linear program $F_N(C)$ to obtain an optimal solution $\mathbf{p}$.
3: Update guess C with $C_N(\mathbf{p})$
4: If $F_N(C) = 0$ then return C else go to Line 2.

B. Dinkelbach-type Algorithm for Optimal Handover

In this section, we consider a simplification of Dinkelbach's algorithm for numerator and denominator coefficients of the objective that are i.i.d. processes. In particular, if we can restrict $\mathbf{p}$ to follow Definition 1, then $\{U_N(\mathbf{p})\}$ and $\{V_N(\mathbf{p})\}$ are i.i.d. processes such that

$$C_{\text{pers}}[\mathsf{H}] = \lim_{N \to \infty} C_N(\mathbf{p}) \qquad (24)$$

by the strong law of large numbers, where $\mathbf{p}$ now corresponds to some valid $\mathsf{H} \in \mathcal{H}$. Under this uncoordinated handover regime, Dinkelbach's solution is asymptotically equivalent to the following optimal handover strategy.

Theorem 2. *The optimal handover strategy chooses a visible satellite from $\mathcal{V}$ with fading parameters determined by S as*

$$\mathsf{H}^*(\mathcal{V}, S) = \argmax_{(\Theta_k, \Phi_k, A_k) \in \mathcal{V}} \left\{ \mathsf{C}(\Theta_k, \Phi_k, A_k) \\ - C_{\text{pers}}[\mathsf{H}^*]\, \mathsf{N}(\Theta_k, \Phi_k, A_k) \right\}. \qquad (25)$$

Proof. Let $Q^{(n)}(C) = \max_{1 \le k \le |\mathcal{V}|} \{ C_{k,n} - C T_{k,n} \}$ and $Q_N(C) = \frac{1}{N} \sum_{n=1}^{N} Q^{(n)}(C)$. Observe that

$$\begin{aligned} Q(C) &= \lim_{N \to \infty} Q_N(C) \\ &= \mathbb{E}_{\mathcal{V}, S} \left[\max_{1 \le k \le |\mathcal{V}|} \{ \mathsf{C}(\Theta_k, \Phi_k, A_k) - C\mathsf{N}(\Theta_k, \Phi_k, A_k) \} \right] \end{aligned} \qquad (26)$$

is an upper bound on $F(C) = \lim_{N \to \infty} F_N(C)$ for uncoordinated handovers. By monotonicity of expectation and since $Q_N(C)$ is monotone decreasing (see Appendix B), $Q(C)$ will converge to zero and coincide with Dinkelbach's solution. $\square$

That is, assuming that the maximum capacity is known, the optimal satellite for handover is selected by maximising the residual between the instantaneous serving capacity and the averaged maximum capacity. To compute the maximum capacity $C_{\text{pers}}[\mathsf{H}^*]$, Dinkelbach's algorithm is modified to obtain the simplified Dinkelbach-type procedure described in Algorithm 2, where the key distinction is that the maximisation is performed over pairs of numerator and denominator terms, rather than jointly over all terms.

The advantage of Algorithm 2 over Algorithm 1 is that it has a per-iteration time-complexity of $O(N)$. However, the number of iterations required for convergence in Algorithm 2 is nontrivial to characterise. If we assume it converges *super-linearly*, as in Algorithm 1, then the overall time-complexity can be approximated as $O(N \log N)$. Based on our numerical evidence, this is a reasonable assumption.

Interestingly, the optimal handover strategy can be applied to more general channel models with arbitrary serving capacity functions C, assuming the capacity limit in (24) exists. For example, we may use it on a deterministic simulation of the satellite mega-constellation over N handovers.

If we wish to have a handover strategy that does not require knowledge of $C_{\text{pers}}[\mathsf{H}^*]$, as in the optimal handover strategy,

---

Algorithm 2 Dinkelbach-type algorithm for estimating $C_{\text{pers}}[\mathsf{H}^*]$

1: Set $C = C_0$ as an initial guess C_0.
2: Solve $Q^{(n)}(C)$, $1 \le n \le N$, to obtain solution $\mathbf{p}$.
3: Update guess C with $C_N(\mathbf{p})$.
4: If $Q_N(C) < \epsilon$ then return C else go to Line 2.

---

then we could instead maximise the capacity over one orbit as in the *max. serving capacity (MSC)* handover strategy [8]

$$\mathsf{H}_{\text{MSC}}(\mathcal{V}, S) = \argmax_{(\Theta_k, \Phi_k, A_k) \in \mathcal{V}} \left\{ \frac{\mathsf{C}(\Theta_k, \Phi_k, A_k)}{\mathsf{N}(\Theta_k, \Phi_k, A_k)} \right\}. \qquad (27)$$

For the case of constant serving times, which arises when $T_{\min} = T_{\max}$, then we have $\mathsf{H}_{\text{MSC}} = \mathsf{H}^*$. Therefore, this series of simplifications shows how the general optimal handover strategy based on the persistent capacity relates to the existing handover strategies in the literature. This highlights the cases in which each of the previously proposed strategies are optimal, depending on the assumptions or requirements of the handover.

C. Non-Persistent Handover

Now let us consider the non-persistent scenario where $C_{\text{pers}}[\mathsf{H}] = C_{\text{non-pers}}[\mathsf{H}]$. This scenario has a constant serving time of 1 sample, and therefore the optimal handover strategy is to maximise the orbit capacity as in the handover strategy

$$\mathsf{H}_{\text{MSC}_0}(\mathcal{V}, S) \\ = \argmax_{(\Theta_k, \Phi_k, \cdot) \in \mathcal{V}} \left\{ \mathbb{E}_{|h_{k,0}|^2} \left[\log \left(1 + \frac{\gamma |h_{k,0}|^2}{d^2(\Theta_k, \Phi_k)} \right) \right] \right\}. \qquad (28)$$

Since there is no orbit trajectory prediction in this scenario, this strategy may be improved by removing the average with respect to the fading coefficients $\{h_{k,0}\}$ if they are assumed to be side-information, since they can theoretically be estimated close to the handover time; this is the handover strategy that was employed in [12]. If the fading coefficients are identical as $h_{1,0} = h_{2,0} = \cdots = h_{N_{\text{vis}},0}$, which coincides with the case of no fading if they equal a constant of 1, then we can equivalently minimise distance as in the nearest-satellite handover strategy; in this scenario, the capacity upper bound in Proposition 1 is the Shannon capacity $\log(1 + \gamma |h_{1,0}|^2 / h^2)$ with a best-case path loss h^2.

D. Worst-Case Handover without Side-Information

As a benchmark for the other more sophisticated handover strategies, we now consider a worst-case handover strategy. Let us restrict the CCU to not be allowed to use any side-information about the visible satellites $\mathcal{V}$ and fading parameters S for making the handover decision. In this scenario, the ordering of the visible satellites in $\mathcal{V}$ is arbitrary and hence the best handover strategy is to choose a random satellite as

$$\mathsf{H}_{\text{Rand}} = \mathcal{U}(\mathcal{V}). \qquad (29)$$

This handover strategy is particularly tractable for analysis since it does not involve order statistics. In fact, the persistent

capacity with this handover strategy can be evaluated via numerical integration using [8, Lemma 1]; for completeness, we summarise this Lemma and its proof in Appendix A. Note that the previous handover strategies include order statistics that make numerical computation of persistent capacity very challenging, unless the serving times are sufficiently short such that it equals the non-persistent capacity from Section IV-C.

Proposition 2. *The persistent capacity is minimised with the random handover strategy such that $C_{\text{pers}}[\text{H}] \geq C_{\text{pers}}[\text{H}_{\text{Rand}}]$ for any handover strategy* H *that satisfies Definition 1.*

Proof. The information-bearing signal that we want to transmit over the persistent satellite channel is denoted by $\mathbf{x}$. Since we are allowed to choose the satellite link, there is an additional channel input that specifies our satellite choice, denoted by the index k. The channel output is denoted by $\mathbf{y}$. Then, ignoring CSI for simplicity, the achievable rate is the mutual information $I(\mathbf{x}, k; \mathbf{y}|\mathcal{V}, S)$, where $(\mathcal{V}, S)$ specifies the side-information available for making the handover decision (i.e., the visible satellite positions and their directions). Since conditioning cannot decrease mutual information [21], we have

$$I(\mathbf{x}, k; \mathbf{y}) \leq I(\mathbf{x}, k; \mathbf{y}|\mathcal{V}, S), \tag{30}$$

which says that any additional side-information cannot degrade the channel. For Gaussian-distributed inputs, mutual information becomes the Shannon capacity. Now, observe that maximising the persistent capacity with respect to the set of handover strategies without side-information gives $C_{\text{pers}}[\text{H}_{\text{Rand}}]$ (that is, no other handover strategy can do better nor worse). Hence, this is a lower bound on the persistent capacity $C_{\text{pers}}[\text{H}]$ for all handover strategies with side-information $(\mathcal{V}, S)$ as in Definition 1. $\square$

VI. NUMERICAL RESULTS

The numerical results to come in this section will compare the handover strategies H_{Rand}, H_{MSC_0}, H_{MSC}, and H^*, as defined in the previous section, in terms of the persistent capacity from Theorem 1. The persistent capacity with H_{Rand} is computed using numerical integration to give a lower bound, which is paired the upper bound from Theorem 1 that is also computed numerically. For the other handover strategies, we use Monte Carlo simulations with 10^3 realisations of the satellite mega-constellation to accurately estimate the persistent capacities. To verify the semi-stochastic model for evaluating handover strategies, we use the Starlink mega-constellation from a TLE file with an epoch date of 2024/01/01, filtering the satellites with parameters that satisfy $b = 53 \pm 1°$ and $h = 550 \pm 50$ km. The mega-constellation is simulated to get satellite positions at $\Delta t = 1$ second intervals, for a duration over 80 hours with SGP4 orbit propagation and for 10 orbital periods with circular orbit (CIRC) propagation. The position data from these simulations is used to estimate the persistent capacities according to the SGP4 and CIRC models for comparison with the theoretical NBPP model. The shadowed-Rician fading model is parameterised using the "average shadowing" parameters from [18, Table III],

which correspond to choosing $S(\theta, \phi; t) = (b_0, m, \Omega) = (0.126, 10.1, 0.835)$.[4] Since the handover strategies are user-centric, we must also choose a ground user location: we study ground users in Melbourne, Australia, and in Helsinki, Finland, which represent distinct locations with a low and a high latitude, respectively.

A. Serving Capacity

Recall that the sub-optimal max. serving capacity handover strategy H_{MSC} maximised the serving capacity $\mathsf{C}(\theta, \phi, a)/\mathsf{N}(\theta, \phi, a)$ over all visible satellite parameters in $\mathcal{V}$, and additionally recall that the persistent capacity could be upper bounded by maximising the serving capacity over $\textsf{Cap}$ (i.e., without the restriction of a finite set of visible satellites). Since the metric for H_{MSC} directly relates to C_{pers}, it is a particularly interesting function to study that provides insights on the qualitative features considered when choosing a serving satellite.

In Fig. 2, the serving capacity for ascending satellites is plotted as a heat map for each ground user without serving time constraints and with a fixed serving time of 15 seconds. For each case, we plot the satellite position with the highest reliability, corresponding to $\overline{C}_{\text{pers}}$. Without serving time constraints in Fig. 2(a) and Fig. 2(b), we observe that the most reliable serving satellites are those that have recently entered the visibility cap and will eventually pass nearby the user; the least reliable satellites are those that are leaving the visibility cap, since they are moving further away from the user. For the fixed serving time in Fig. 2(c) and Fig. 2(d), we observe that the serving capacity follows $\sigma(\theta, \phi) \propto d(\theta, \phi)$, with a slight skew towards the bottom-left due to the persistence introduced by the 15-second serving time. This may be viewed as a visual proof that such short durations are almost without persistence, and thus we can essentially just choose the nearest satellite. Note that the shadowing model is not causing additional skewing in this example, since the shadowing parameters chosen for S are independent of (θ, ϕ).

B. Persistent Capacity without Serving Time Constraints ($T_{\min} = 0$, $T_{\max} = \infty$)

Let us now consider the case of unconstrained serving times, which corresponds to a minimum serving time $T_{\min} = 0$ and a maximum serving time $T_{\max} = \infty$. In this scenario, the only constraint is that we can only be served for the serving satellite's visibility time as $T_{\text{serv}} = T_{\text{vis}}(\Theta_0, \Phi_0, A_0)$, i.e., while the satellite is in the visibility cap. The motivation for studying this scenario is that it results in long serving times (low handover rate) since the satellite persistence is high. Since this results in variable serving times, it is a key example for demonstrating the performance of H^* relative to the other sub-optimal handover strategies.

In terms of modelling accuracy, Fig. 3 shows a close agreement between the persistent capacities for NBPP, SGP4

---

[4]Alternatively, we could upgrade the model to include time-dependent satellite positions using [18, Eq. 19] to get $S(\theta(t), \phi(t), t) = (b_0(\sigma(t)), m(\sigma(t)), \Omega(\sigma(t)))$. We omit this here to keep our results comparable with results in the literature.
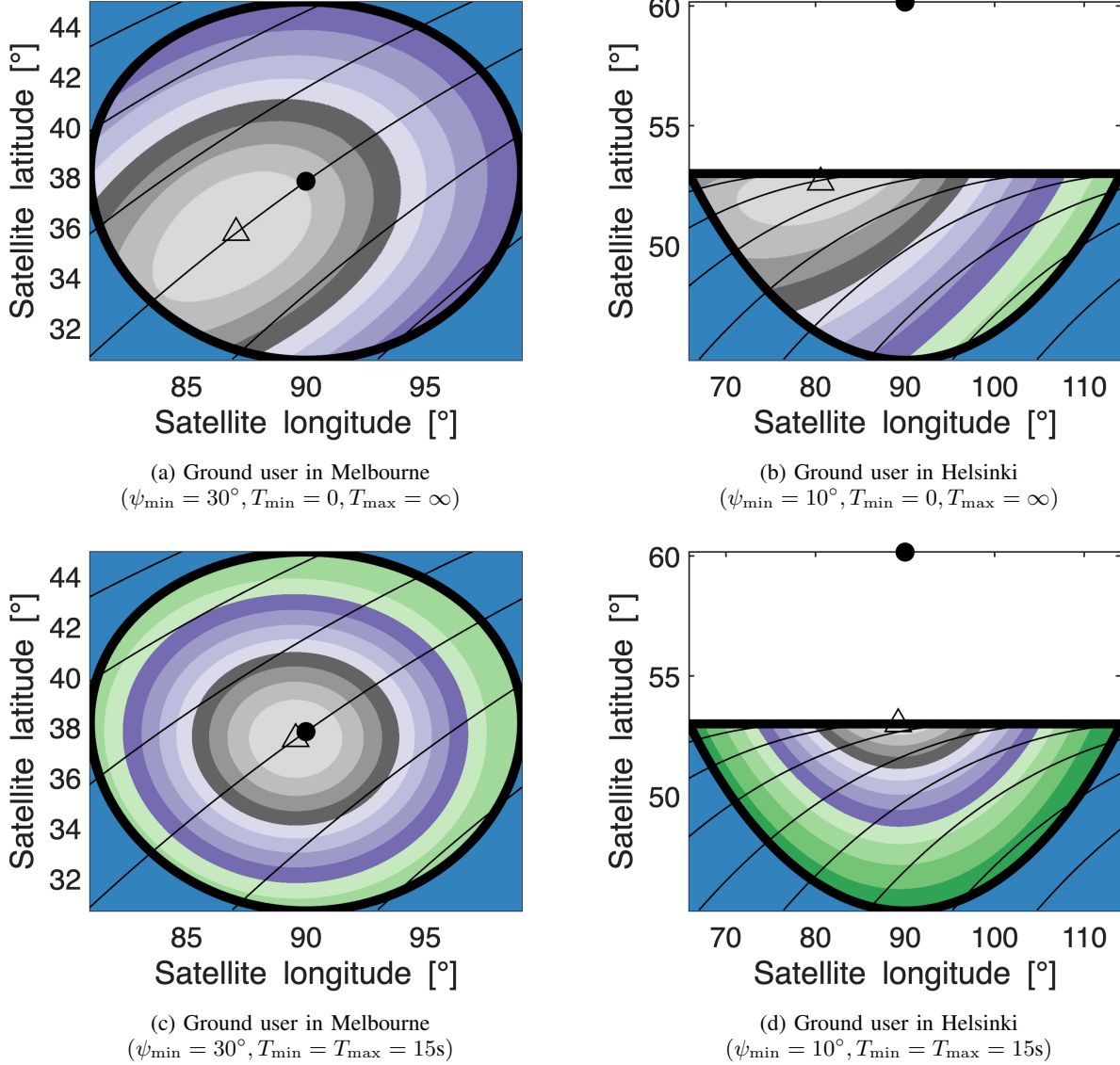
Figure 2: Heat maps of the serving capacity $C(\theta, \phi, 1)/N(\theta, \phi, 1)$ for ascending satellites. Light grey is the highest serving capacity, dark green is the lowest serving capacity, and blue (and white) is zero capacity (outside the visibility cap). The black dot is the location of the ground user, the triangle marker is the satellite location that achieves the capacity upper bound $\overline{C}_{\text{pers}}$, the thin black lines are example orbit trajectories, and the thick black curve is the boundary of the visibility cap Cap.

and CIRC. This supports the accuracy of the semi-stochastic model and suggests the handover independence assumption is a reasonable approximation. However, $C_{\text{pers}}[\mathsf{H}^*]$ exhibits the least agreement between NBPP and SGP4/CIRC, as observed for the user in Melbourne, who actually has a lower capacity with H^* than with H_{MSC}. This indicates that the performance gain of H^* over H_{MSC} is unlikely to be practically significant. In addition, it is interesting to note that $C_{\text{pers}}[\mathsf{H}_{\text{Rand}}]$ has the closest model agreement for both users. We briefly note that Algorithm 2 converges within five iterations for these examples.

Comparing the handover strategies in Fig. 3, we confirm that the handover strategies with more side-information have higher persistent capacities for both users. For both users,

$\mathsf{H}_{\text{MSC}_0}$ has a gain of $\{0.62, 0.67\}$ dB over H_{Rand}, H_{MSC} has a gain of $\{0.38, 0.45\}$ dB over $\mathsf{H}_{\text{MSC}_0}$, and H^* has a gain of $\{0.07, 0.03\}$ dB over H_{MSC}. Overall, the optimal handover strategy has a gain of $\{1.07, 1.15\}$ dB compared to the worst-case handover strategy. That is, by using all of the available information in the handover strategy, we have effectively increased the transmit power by more than 1 dB for both users.

The capacity upper bound $\overline{C}_{\text{pers}}$ in Proposition 1 is observed to be tight in Fig. 3, suggesting that there is often a visible satellites in the light grey regions of their respective heat maps in Fig. 2(a) and 2(b). In addition, the bound is especially tight for the higher latitude user since the density of satellites according to $f_\Phi(\phi)$ is higher. For such serving times, this
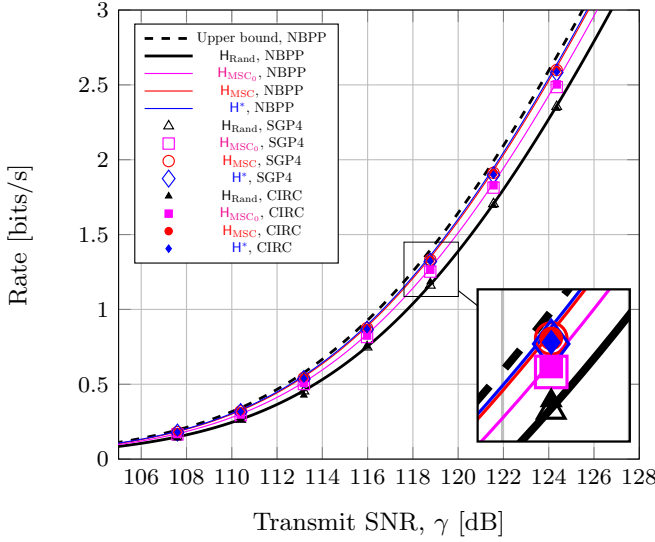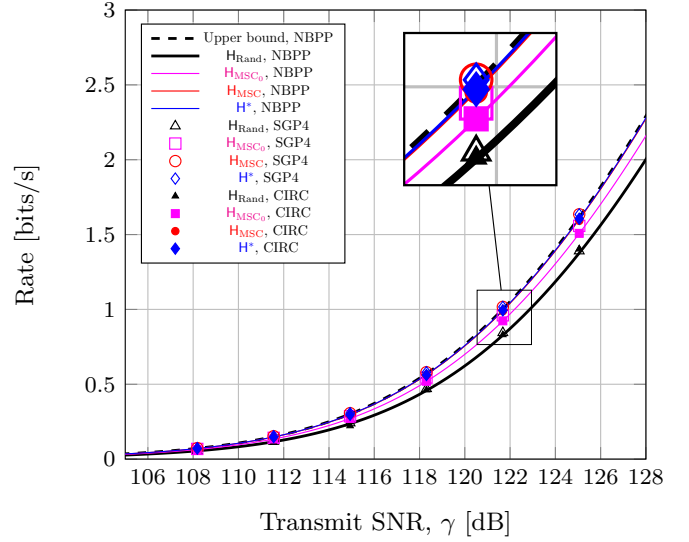
(a) Ground user in Melbourne ($\psi_{\min} = 30°$)

(b) Ground user in Helsinki ($\psi_{\min} = 10°$)

Figure 3: Persistent capacity with cap serving times for a range of transmit SNRs.

upper bound may actually be sufficiently tight for use in a simplified theoretical analysis.

C. Persistent Capacity with Fixed Serving Times ($T_{\min} = T_{\max}$)

Let us now consider the case of fixed serving times, which corresponds to constraining the minimum and maximum serving times as $T_{\min} = T_{\max} = T_{\text{serv}}$ where T_{serv} is now a constant that we can set. Unlike with the cap serving times, in this scenario H^* coincides with H_{MSC} since the serving times are constant. A strong motivation for studying fixed serving times is that the Starlink mega-constellation network is known to perform inter-satellite handovers every 15 seconds [24], which are synchronised to occur at the 12th, 27th, 42nd, and 57th second past every minute for all users.

As earlier, we observe in Fig. 4 that the persistent capacities for all handover strategies remain in close agreement between NBPP, SGP4, and CIRC with the additional constraint of fixed serving times. We note that the data points for SGP4 and CIRC with longer serving times are less accurate, since there are less handovers over the same simulation period to average over, but this appears to be insignificant in the results.

As expected, we observe in Fig. 4 that H_{MSC_0} and H_{MSC} have an equal persistent capacity for short serving times, which is 1.8442 bits/s in Melbourne and reduces to 1.5145 bits/s in Helsinki due to the higher latitude. In addition, H_{Rand} degrades the capacity with H_{MSC} by 0.4828 bits/s in Melbourne and by a similar 0.4837 bits/s in Helsinki. An important observation from these numerical results is that the difference between H_{MSC} and H_{MSC_0} remains unnoticeable for serving times up to 10–20 seconds, characterising the sensitivity of the handover strategy to persistence. For longer serving times, H_{MSC} outperforms both H_{MSC_0} and H_{Rand} by a growing margin, since they do not use any information regarding the orbit trajectory over the serving time; when the serving time is short, there is relatively little information to use for handover, however, as the serving time increases, there is more and more information that must be used to make the most informed decision possible—this is why long serving times result in more complicated handover strategies compared to those for short serving times.

The capacity upper bound $\overline{C}_{\text{pers}}$ is significantly looser with fixed serving times compared to the earlier case with cap serving times. This may be justified through their respective heat maps in Fig. 2(c) and Fig. 2(d), which show significantly smaller light grey regions, reducing the probability of a visible satellite with a capacity near the upper bound. Nonetheless, the higher latitude user has a tighter bound, and in this scenario the bound is significantly tighter than at lower latitudes.

From our additional simulations, we observe that the effects of varying the minimum elevation angle and fading parameters are consistent with theoretical predictions. Reducing the elevation angle threshold $\psi_{\min}$ enlarges the satellite visibility cap, resulting in higher capacities for the optimal handover strategy, while the random strategy degrades due to the inclusion of lower-elevation satellites. In contrast, heavier shadowing conditions reduce overall capacities and the variability across elevation angles is diminished. As a result, the advantage of choosing higher-elevation satellites is reduced, and the performance gap between the random and optimal handover strategies narrows. We expect these observations to hold for arbitrary serving times.

VII. CONCLUSION

This paper introduced persistent capacity for a semi-stochastic mega-constellation channel model to investigate optimal handover strategies for general serving times, extending prior stochastic models that were limited to short serving times. Persistent capacity accurately characterises the capacity of LEO satellite networks for a fixed ground user, and
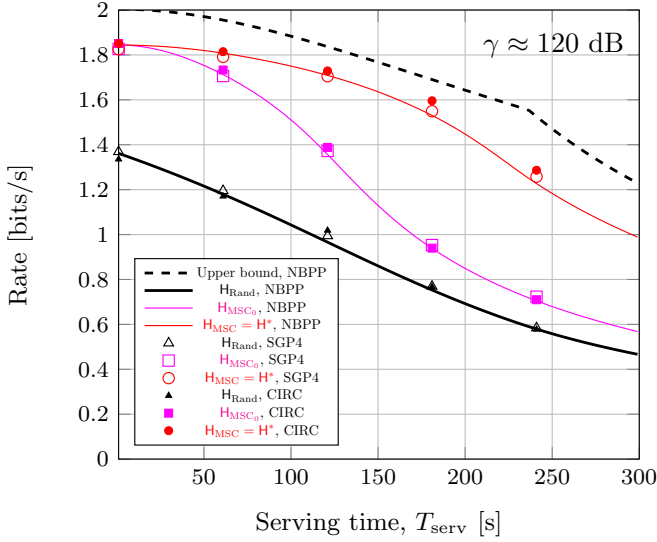
(a) Ground user in Melbourne ($\psi_{\min} = 30°$)
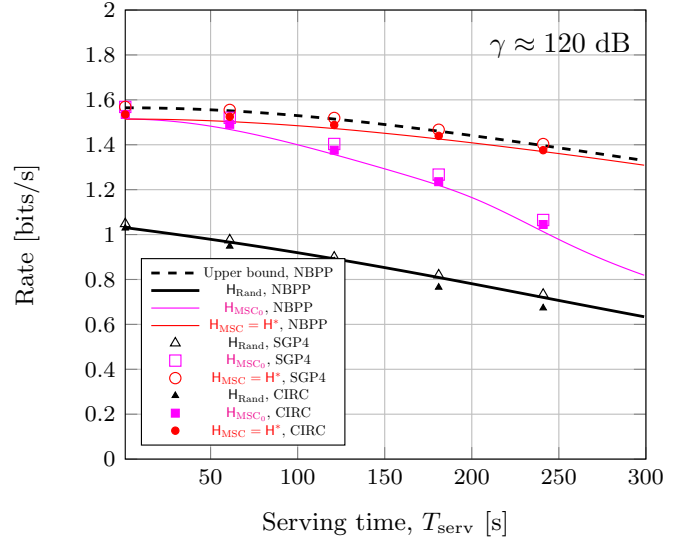
(b) Ground user in Helsinki ($\psi_{\min} = 10°$)

Figure 4: Persistent capacity for a range of fixed serving times and a fixed transmit SNR $\gamma \approx 120$ dB.

the optimal handover strategy that maximises it was derived using a Dinkelbach-type algorithm for non-linear fractional programs. This yields a tractable closed-form decision rule that induces an ordering over preferred satellites for handover, which can be exploited in multi-user handover optimisation algorithms to reduce the search space and simplify large-scale assignment problems [11].

Numerical results showed that non-persistent capacity approximates persistent capacity well for serving times up to around 15 seconds, consistent with current Starlink operations, while longer serving times require the optimal strategy to avoid significant capacity degradation. Tight information-theoretic upper and lower bounds were derived to address the cases known to be intractable, with the upper bound particularly accurate for high-latitude users. Extensions to account for limited resources (via *thinning* the point process), interference (via additional noise terms), or time-varying fading (via *Markov* renewal models) are straightforward and preserve the tractable optimal handover strategy. The framework can also be extended to emerging multi-layer NTN architectures, such as integrated LEO and MEO constellations, and to air-to-space communications, provided that orbit predictions or position knowledge are sufficiently accurate to enable the use of persistent capacity. Such extensions may facilitate integration into future 6G-NTN standardisation contexts.

Overall, this information-theoretic framework establishes a true upper limit on achievable coding rates in LEO satellite networks and identifies practical handover strategies that attain it, significantly advancing the design and analysis of large-scale user-satellite communication systems.

APPENDIX

A. Closed-Form Persistent Capacity for Random Handover

Let $\Delta t \to 0$ so that the persistent capacity with random handover can be written as[5] [8]

$$C_{\text{pers}}[\mathsf{H}_{\text{Rand}}] = \frac{\mathbb{E}\left[\mathsf{C}_t(\Theta, \Phi, A)\right]}{\mathbb{E}[T_{\text{serv}}(\Theta, \Phi, A)]} \tag{31}$$

where

$$\mathsf{C}_t(\Theta, \Phi, A) = \int_0^{T_{\text{serv}}(\Theta, \Phi, A)} \mathbb{E}_{|h(t)|^2}\left[\log\left(1 + \frac{\gamma|h(t)|^2}{d^2(\Theta(t), \Phi(t))}\right)\right] dt \tag{32}$$

for shadowed-Rician process $h(t)$, which is readily computable using numerical integration.

The integration for computing the expectation $\mathbb{E}[f(\Theta, \Phi, A)]$ for each function $f \in \{\mathsf{C}_t, T_{\text{serv}}\}$ over the cap region Cap is [8]

$$\mathbb{E}[f(\Theta, \Phi, A)] = \frac{1}{4\pi} \int_0^\pi \int_{\theta_L(\phi)}^{\theta_U(\phi)} [f(\theta, \phi, -1) + f(\theta, \phi, 1)] f_\Phi(\phi) d\theta d\phi. \tag{33}$$

Therefore, the persistent capacity with random handover can be computed using numerical integration.

B. Properties of $Q_N(C)$

Lemma 1. $Q_N(C)$ *is convex.*

---

[5]Note that this is a tight approximation for any finite Δt within the coherence time of the satellite path loss.

Proof. For $t \in [0,1]$ and $C, C' \in \mathbb{R}$, we have

$$
\begin{aligned}
Q_N(tC + (1-t)C') &= \frac{1}{N} \sum_{n=1}^{N} \max_{1 \le k \le |\mathcal{V}|} \big\{ t(C_{k,n} - CT_{k,n}) \\
&\quad + (1-t)(C_{k,n} - C'T_{k,n}) \big\} \\
&\le \frac{t}{N} \sum_{n=1}^{N} \max_{1 \le k \le |\mathcal{V}|} \{ C_{k,n} - CT_{k,n} \} \\
&\quad + \frac{1-t}{N} \sum_{n=1}^{N} \max_{1 \le k \le |\mathcal{V}|} \{ C_{k,n} - C'T_{k,n} \} \\
&= tQ_N(C) + (1-t)Q_N(C')
\end{aligned}
\tag{34}
$$

$\square$

Lemma 2. $Q_N(C) < Q_N(C')$ *if* $C > C'$.

Proof. For $C, C' \in \mathbb{R}$ with $C > C'$, then for some $k(n)$ we have

$$
Q_N(C) = \frac{1}{N} \sum_{n=1}^{N} (C_{k(n),n} - CT_{k,n}) \tag{35}
$$

$$
< \frac{1}{N} \sum_{n=1}^{N} (C_{k(n),n} - C'T_{k,n}) \tag{36}
$$

$$
\le \frac{1}{N} \sum_{n=1}^{N} \max_{1 \le k \le |\mathcal{V}^{(n)}|} \{ C_{k,n} - C'T_{k,n} \} = Q_N(C'). \tag{37}
$$

$\square$

Lemma 3. $Q_N(C^*) = 0$ *has a unique solution* C^*.

Proof. The result holds since $Q_N(C)$ is convex and monotone decreasing. $\square$

REFERENCES

[1] W. Liu, N. Xiao, B. Liu, and Y. Zhang, "Research on user access technologies in satellite communication networks," in *4th International Conference on Electronic Information Engineering and Computer Communication (EIECC)*, 2024, pp. 235–241.

[2] I. F. Akyildiz, M. D. Bender, and H. Uzunalioglu, "Handover management in low Earth orbit (LEO) satellite networks," *Mobile Networks and Applications*, vol. 4, no. 4, pp. 301–310, December 1999.

[3] Z. Liu, Z. Yang, G. Pan, H. Zhang, G. Luo, and H. Yang, "Handover technique in LEO satellite networks: A review," in *13th International Conference on Communications, Circuits and Systems (ICCCAS)*, 2024, pp. 364–369.

[4] P. K. Chowdhury, M. Atiquzzaman, and W. Ivancic, "Handover schemes in satellite networks: state-of-the-art and future research directions," *IEEE Communications Surveys & Tutorials*, vol. 8, no. 4, pp. 2–14, 2006.

[5] I. del Portillo, B. G. Cameron, and E. F. Crawley, "A technical comparison of three low Earth orbit satellite constellation systems to provide global broadband," *Acta Astronautica*, vol. 159, pp. 123–135, 2019.

[6] N. Okati, T. Riihonen, D. Korpi, I. Angervuori, and R. Wichman, "Downlink coverage and rate analysis of low Earth orbit satellite constellations using stochastic geometry," *IEEE Transactions on Communications*, vol. 68, no. 8, pp. 5120–5134, 2020.

[7] N. Okati and T. Riihonen, "Nonhomogeneous stochastic geometry analysis of massive LEO communication constellations," *IEEE Transactions on Communications*, vol. 70, no. 3, pp. 1848–1860, 2022.

[8] B. McBain, Y. Hong, and E. Viterbo, "Coherent capacity of satellite mega-constellations with persistence," *IEEE International Conference on Communications (ICC)*, June, 2025.

[9] A. M. Voicu, A. Bhattacharya, and M. Petrova, "Handover strategies for emerging LEO, MEO, and HEO satellite networks," *IEEE Access*, vol. 12, pp. 31 523–31 537, 2024.

[10] E. Papapetrou, S. Karapantazis, G. Dimitriadis, and F.-N. Pavlidou, "Satellite handover techniques for LEO networks," *International Journal of Satellite Communications and Networking*, vol. 22, no. 2, pp. 231–245, 2004. [Online]. Available: https://onlinelibrary.wiley.com/doi/abs/10.1002/sat.783

[11] Z. Wu, F. Jin, J. Luo, Y. Fu, J. Shan, and G. Hu, "A graph-based satellite handover framework for LEO satellite communication networks," *IEEE Communications Letters*, vol. 20, no. 8, pp. 1547–1550, 2016.

[12] N. Okati and T. Riihonen, "Coverage and rate analysis of mega-constellations under generalized serving satellite selection," in *IEEE Wireless Communications and Networking Conference (WCNC)*, 2022, pp. 2214–2219.

[13] Y. Guo, C. Skouroumounis, S. Chatzinotas, and I. Krikidis, "On user association in large-scale heterogeneous LEO satellite network," *IEEE Transactions on Aerospace and Electronic Systems*, vol. 60, pp. 5994–6010, 2024.

[14] D. Kim and J. P. Choi, "A reliable handover strategy with second satellite selection in LEO satellite networks," in *2023 IEEE Globecom Workshops*, 2023, pp. 293–298.

[15] H. Feng and L. Zhu, "Handover scheme in LEO satellite networks based on QoE for streaming media services," *Sensors*, vol. 25, no. 7, 2025. [Online]. Available: https://www.mdpi.com/1424-8220/25/7/2165

[16] B. Mcbain, Y. Hong, and E. Viterbo, "Stochastic channel models for satellite mega-constellations," *IEEE Transactions on Communications*, pp. 1–1, 2025.

[17] N. Okati and T. Riihonen, "Stochastic analysis of satellite broadband by mega-constellations with inclined LEOs," in *IEEE 31st Annual International Symposium on Personal, Indoor and Mobile Radio Communications (PIMRC)*, 2020, pp. 1–6.

[18] A. Abdi, W. Lau, M.-S. Alouini, and M. Kaveh, "A new simple model for land mobile satellite channels: first- and second-order statistics," *IEEE Transactions on Wireless Communications*, vol. 2, no. 3, pp. 519–528, 2003.

[19] M. Di Renzo, F. Graziosi, and F. Santucci, "Channel capacity over generalized fading channels: A novel MGF-based approach for performance analysis and design of wireless communication systems," *IEEE Transactions on Vehicular Technology*, vol. 59, no. 1, pp. 127–149, 2010.

[20] E. Biglieri, J. G. Proakis, and S. Shamai, "Fading channels: Information-theoretic and communication aspects," *IEEE Trans. Inf. Theory*, vol. 44, pp. 2619–2692, 1998.

[21] T. M. Cover and J. A. Thomas, *Elements of Information Theory*, 2005.

[22] T. Matsui, Y. Saruwatari, and Maiko, "An analysis of Dinkelbach's algorithm for 0-1 fractional programming problems," 1992.

[23] W. Dinkelbach, "On nonlinear fractional programming," *Management Science*, vol. 13, pp. 492–498, 1967.

[24] J. Zhao and J. Pan, "Low-latency live video streaming over a low-Earth-orbit satellite network with DASH," ser. MMSys '24. New York, NY, USA: Association for Computing Machinery, 2024, p. 109–120. [Online]. Available: https://doi.org/10.1145/3625468.3647616